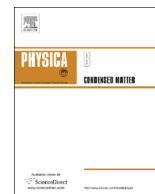




ELSEVIER

Contents lists available at ScienceDirect

Physica B

journal homepage: www.elsevier.com/locate/physb

Molecular dynamics study of melting curve, entropy of fusion and solid–liquid interfacial energy of cobalt under pressure

Wen-jin Zhang^a, Yu-feng Peng^a, Zhong-li Liu^{b,*}^a College of Physics and Electronic Engineering, Henan Normal University, Xinxiang 453007, China^b College of Physics and Electric Information, Luoyang Normal University, Luoyang 471002, China

ARTICLE INFO

Article history:

Received 30 July 2013

Received in revised form

21 December 2013

Accepted 13 January 2014

Available online 21 January 2014

Keywords:

Melting curve

Entropy of fusion

Solid–liquid interfacial energy

Equation of state

Molecular dynamics method

ABSTRACT

We performed molecular dynamics (MD) simulations with the two embedded atom method (EAM) potentials to calculate the melting curves of cobalt over a wide range of pressure. Zhou's EAM potential can produce satisfying results, in better agreement with the experiment compared with Pun's. Based on Zhou's potential, we simulated the melting of Co with two approaches, i.e., the one-phase (hysteresis) method and two-phase (solid–liquid coexistence) method. Both approaches can effectively reduce the superheating, and their results are in the close proximity at the applied pressures. With the one-phase method, during the investigation of the entropy of fusion of Co, we found that with the pressure increasing, the entropy of fusion decreases rapidly first and then oscillates with pressure; when the pressure is beyond 100 GPa, the entropy of fusion shows less pressure effect. When taking account of the solid–liquid interfacial energy at different pressures, we found that it increases monotonically with pressure, and can be well described as a fifth-order polynomial relation. Moreover, the thermal equation of state (EOS) and the temperature dependence of atomic structures of Co have been obtained successfully.

© 2014 Elsevier B.V. All rights reserved.

1. Introduction

Melting properties are of fundamental importance for understanding the equilibrium properties of both solid and liquid phases of materials, and the competition between them. Over the past decade, extensive experimental [1–9] and theoretical studies [10–20] have been focused on the melting properties of a number of transition metals. Particularly, for Fe, its melting properties have attracted much attention [21–29] because its melting, under extreme conditions, could be used to determinate the temperature at the Earth's inner–outer core boundary, which is crucial to constrain the geophysical and geochemical models for the Earth's core. However, accurate determination for the equilibrium melting points of the transition metals is still a challenge to both experimental and theoretical researches. Hence, there exist large discrepancies in the melting curves of transition metals among laser-heated diamond-anvil cell (DAC) measurements [3,30–37], shock wave experiments [35–37] and theoretical simulations [13,20,38,39]. And such discrepancies and therein causes are still under further investigations.

The cobalt element, which is adjacent to iron in the periodic table, is potentially important to understand the properties of the Earth's core that is believed to consist of iron-dominated alloys with Co or Ni as minor components. Furthermore, the structural behavior of Co metal at high pressure and high temperature may shed light on the phase diagram of iron in general. Therefore, the structure, magnetism and elastic properties of cobalt under high pressure have drawn extensive attention [40–49]. Unfortunately, the studies of its melting properties are rare up to now. There is a significant disagreement between the existing high-pressure experimental melting points of Co [31,50]. This motivates us to investigate the high-pressure melting curve of Co.

Bulk cobalt metal has two solid phases. The hexagonal close-packed (hcp) α phase is stable at ambient conditions. The face-centered-cubic (fcc) β phase exists at high temperature above 693 K, and can be quenched to ambient conditions as a metastable phase [40]. Under compression above 100 GPa, hcp cobalt also transforms into fcc structures at room temperature [44]. Cobalt melts from fcc [31,51] at pressure. Thus in present work, we treat fcc phase as the unique phase from which solid Co melts within the whole range of pressure of interest.

Presently, several methods have been developed for the computation of melting points of crystals. These methods can be categorized into two groups. The first group, which will be referred to as “direct” methods, include the superheating–supercooling hysteresis (one-phase) method [52], the solid–liquid coexistence (two-phase)

* Corresponding author. Tel./fax: +86 379 655 150 16.

E-mail addresses: wjzhr@yeah.net (W.-j. Zhang), zhonglilium@yeah.net (Z.-l. Liu).

method [53], and the Z method [54]. In the one-phase method, the solid phase is heated incrementally until melt at fixed pressure, and then the obtained liquid phase is cooled until freezing. The melting temperature is deduced from the temperatures of overheating and undercooling [29,55–60]. In the two-phase method, the MD simulations are performed on supercells containing a solid–liquid interface, and overheating could be overcome [10,15,16,20,61–63]. In the Z method, the calculation is carried out in NVE ensemble (number of atoms N , volume V , and energy E) where the simulated initial configuration is solid, and the whole processes lie on the isochore curve. With the temperature increasing, the solid melts spontaneously to reach the critical overheating T_{ls} and then the temperature drops to the melting temperature T_m [18,64,65]. The second category of the method will be referred to as the free energy method. This method is based on the calculation of the Gibbs free energies of both solid and liquid phases, and the melting temperature T_m at a given pressure P can be found from the equality $G_{liq}(P, T_m) = G_{solid}(P, T_m)$ in thermodynamic equilibrium [66–68]. In these approaches, the melting curves are determined by the selected potential forms and potential parameters. Different potential forms and potential parameters could produce different melting curves. Most potential parameters were fitted to solid phase only, however, if they were fitted to both solid and liquid phases simultaneously, one could correctly reproduce the melting curves of materials. In this work, we investigated melting properties of cobalt using MD simulations with two EAM potentials [51,69].

The rest of the paper is organized as follows: in Section 2, the theoretical methods and calculation details are described. The results and discussions are presented in Section 3. The short conclusions are summarized in Section 4.

2. Theoretical methods and calculation details

2.1. Potential functions

For molecular dynamics simulations of melting of cobalt, we have adopted two EAM potentials to compare which one is appropriate to simulate the melting properties of cobalt at high pressures and high temperatures. There are some form differences between the two potentials. The first potential was recently constructed by Pun and Mishin [51] based on the fcc and hcp structures of Co, in which the total energy of a collection of atoms can be written as follows:

$$E = \frac{1}{2} \sum_{ij} \phi(r_{ij}) + \sum_i F(\bar{\rho}_i), \quad (1)$$

where $\phi(r_{ij})$ is a pair-interaction potential as a function of distance r_{ij} between atoms i and j , and $F(\bar{\rho}_i)$ is the embedding energy as a function of the host electron density $\bar{\rho}_i$ on atom i . The host electron density,

$$\bar{\rho}_i = \sum_{k \neq i} \rho(r_{ik}), \quad (2)$$

is the sum of atomic electron densities created at site i by all other atoms of the system. In this potential, the pair interactions are described by the generalized Lennard–Jones-type function,

$$\phi(r) = \psi \left(\frac{r-r_c}{h} \right) \left[\frac{V_0}{b_2-b_1} \left(\frac{b_2}{(r/r_1)^{b_1}} - \frac{b_1}{(r/r_1)^{b_2}} \right) + \delta \right], \quad (3)$$

where r_c , h , V_0 , b_1 , b_2 , r_1 and δ are fitting parameters. This function is smoothly truncated at the cutoff distance $r=r_c$ using the truncation function,

$$\psi(x) = \begin{cases} \frac{x^4}{1+x^4}, & x < 0 \\ 0, & x \geq 0. \end{cases} \quad (4)$$

The analytical form of the electron-density function is chosen to be

$$\rho(r) = \psi \left(\frac{r-r_c}{h} \right) [A_0 z^y \exp^{-\gamma z} (1 + B_0 \exp^{-\gamma z}) + C_0], \quad (5)$$

where $z=r-r_0$ with the parameters A_0 , y , γ , B_0 , C_0 and r_0 . All parameter values are taken from Ref. [51].

The second potential is an EAM alloy potential model [69]. In this model, the total energy E of the crystal can be written as

$$E = \frac{1}{2} \sum_{i,j,i \neq j} \phi_{ij}(r_{ij}) + \sum_i F_i(\rho_i), \quad (6)$$

where ϕ_{ij} stands for the pair energy between atom i and j separated by a distance r_{ij} , and F_i represents the embedding energy to embed an atom i into a local site with an electron density ρ_i . The electron density can be expressed as

$$\rho_i = \sum_{ij,j \neq i} f_j(r_{ij}) \quad (7)$$

where $f_j(r_{ij})$ is the electron density at the site of atom i arising from atom j at a distance r_{ij} away. To fit such an EAM set, the generalized pair potentials are chosen to have the following form:

$$\phi(r) = \frac{A \exp[-\alpha(r/r_e - 1)]}{1 + (r/r_e - \kappa)^{20}} - \frac{B \exp[-\beta(r/r_e - 1)]}{1 + (r/r_e - \lambda)^{20}}, \quad (8)$$

where r_e is the equilibrium spacing between nearest neighbors, A , B , α and β are four adjustable parameters, and κ and λ are two additional parameters for the cutoff. The electron density function is taken with the same form as the attractive term in the pair potential, i.e.,

$$f(r) = \frac{f_e \exp[-\beta(r/r_e - 1)]}{1 + (r/r_e - \lambda)^{20}}. \quad (9)$$

To have embedding energy functions that can work well over a wide range of electron density, three equations are used to separately fit three different electron density ranges. These equations are

$$F(\rho) = \sum_{i=0}^3 F_{ni} \left(\frac{\rho}{\rho_n} - 1 \right)^i, \quad \rho < \rho_n, \quad \rho_n = 0.85\rho_e, \quad (10)$$

$$F(\rho) = \sum_{i=0}^3 F_i \left(\frac{\rho}{\rho_e} - 1 \right)^i, \quad \rho_n \leq \rho < \rho_0, \quad \rho_0 = 1.15\rho_e, \quad (11)$$

$$F(\rho) = F_e \left[1 - \ln \left(\frac{\rho}{\rho_s} \right)^\eta \right] \left(\frac{\rho}{\rho_s} \right)^\eta, \quad \rho_0 \leq \rho. \quad (12)$$

The parameters for cobalt are shown in previous work by Zhou et al. [69].

Both of the above potentials can reliably reproduce some of the basic physical properties of hcp and fcc cobalt at zero pressure, including the lattice constants, cohesive energies, elastic constants, vacancy formation and migration energies, stacking faults, surface energies, and thermal expansion. However, the high pressure behaviors of two potentials are necessary to be further investigation.

2.2. Molecular dynamics simulations

All MD simulations were carried out using LAMMPS package [70] with period boundary conditions. A time step of 1 fs was used to perform the integration of the equation of motion and the smooth particle mesh Ewald method [71] was employed with the electrostatic interaction. The Nose–Hoover thermostat and barostat method [72] was applied to control the temperature and pressure. The relaxation times used for the thermostat and barostat are 30 ps, respectively. The system was equilibrated for

Download English Version:

<https://daneshyari.com/en/article/1809624>

Download Persian Version:

<https://daneshyari.com/article/1809624>

[Daneshyari.com](https://daneshyari.com)